

Uncertainty is Maintained and Used in Working Memory

Aspen H. Yoo^{1,2,3}, Luigi Acerbi^{1,2,4}, Wei ji Ma^{1,2}

Department of Psychology, New York University, NY, USA¹

Center for Neural Science, New York University, NY, USA²

Department of Psychology, University of California, Berkeley, CA, USA³

Department of Computer Science, University of Helsinki, Helsinki, Finland⁴

Funding: This work was supported by NIH grant R01EY020958 to W.J.M. and training grant T32 EY7136-25 to A.H.Y.

1 Abstract

2 What are the contents of working memory? In both behavioral and neural computational models, a working memory
3 representation is typically described by a single number, namely a point estimate of a stimulus. Here, we asked if peo-
4 ple also maintain the uncertainty associated with a memory, and if people use this uncertainty in subsequent decisions.
5 We collected data in a two-condition orientation change detection task; while both conditions measured whether peo-
6 ple used memory uncertainty, only one required maintaining it. For each condition, we compared an optimal Bayesian
7 observer model, in which the observer uses an accurate representation of uncertainty in their decision, to one in which
8 the observer does not. We find that this “Use Uncertainty” model fits better for all participants in both conditions. In
9 the first condition, this result suggests that people use uncertainty optimally in a working memory task when that un-
10 certainty information is available at the time of decision, confirming earlier results. Critically, the results of the second
11 condition suggest that this uncertainty information was maintained in working memory. We test model variants and
12 find that our conclusions do not depend on our assumptions about the observer’s encoding process, inference process,
13 or decision rule. Our results provide evidence that people have uncertainty that reflects their memory precision on an
14 item-specific level, maintain this information over a working memory delay, and use it implicitly in a way consistent
15 with an optimal observer. These results challenge existing computational models of working memory to update their
16 frameworks to represent uncertainty.

17
18 Keywords: visual working memory, Bayesian observer, optimal, uncertainty

19 2 Introduction

20 Visual working memory, the process involved in actively maintaining visual information over a short period, is essen-
21 tial for numerous everyday behaviors as “simple” as integrating visual information across saccades and as “complex”
22 as reading comprehension, problem solving, and decision making (Baddeley & Hitch, 1974; Baddeley, 2003; Fukuda,
23 Vogel, Mayr, & Awh, 2010; Conway, Kane, & Engle, 2003; Just & Carpenter, 1992). As important as it is, visual
24 working memory is also a notoriously limited process, resulting in an imperfect and incomplete picture of the world it
25 aims to represent.

26 Both behavioral (e.g., Zhang & Luck, 2008; Bays & Husain, 2008; van den Berg, Shin, Chou, George, & Ma, 2012;
27 Fougnie, Suchow, & Alvarez, 2012) and neural (e.g., Ermentrout, 1998; Wang, 2001; Compte, 2006) models of visual
28 working memory typically represent people’s memory as a single number, a noisy estimate of the value of the stimulus.
29 For example, someone may remember a 34° oriented line as 37°. It is, however, important in many visual working
30 memory decisions to represent more than just a point estimate of the remembered stimulus, but the uncertainty as well.
31 Uncertainty is technically defined as the width of a belief distribution over a stimulus, but intuitively is a subjective
32 measure representing how unsure an observer is about the stimulus. This is different from memory precision, which is
33 objective and represents how precisely an observer actually remembers the stimulus. An ideal observer’s uncertainty
34 will reflect the precision with which they remembered an item, such that they are less uncertain for more precise
35 memories. They will use this knowledge by weighing low-uncertainty information more heavily than high-uncertainty
36 information. In a variety of domains, this strategy would increase performance and thus should be used. For example,
37 high uncertainty over the memory of the location of a coffee cup may result in someone looking at it before reaching
38 for it. High uncertainty over whether a friend changed their appearance may result in someone being less likely to
39 comment on it.

40 Does uncertainty get taken into account in working memory-based decisions? An intuitive first place to look
41 is the literature on working memory confidence, since confidence can be thought of as a readout of uncertainty.
42 Experimenters have probed memory confidence by asking people to provide a rating (Rademaker, Tredway, & Tong,
43 2012; Vandenbroucke et al., 2014; Samaha & Postle, 2017), choose the best remembered item (Fougnie et al., 2012;
44 Suchow, Fougnie, & Alvarez, 2017), or make a memory-based bet (Yoo, Klyszejko, Curtis, & Ma, 2018; Honig,
45 Ma, & Fougnie, 2020). These studies have demonstrated that people have higher working memory confidence on
46 trials that are remembered more accurately (but see Sahar, Sidi, & Makovski, 2020; Bona, Cattaneo, Vecchi, Soto,
47 & Silvanto, 2013; Bona & Silvanto, 2014; Vlassova, Donkin, & Pearson, 2014; Maniscalco & Lau, 2015; Adam &
48 Vogel, 2017; Samaha, Barrett, Sheldon, LaRocque, & Postle, 2016 for conflicting results), and a computational model
49 in which memory judgements and confidence ratings are derived from the same underlying memory precision can
50 quantitatively account for these joint data (van den Berg, Yoo, & Ma, 2017).

51 All these studies ask the participant to consciously access the quality of their memory. However, in naturalistic
52 settings, people are typically not directly interrogated about their uncertainty, but use it implicitly in order to benefit
53 later decisions. For example, looking before reaching for one’s coffee cup or commenting on a friend’s appearance are
54 decisions that presumably use uncertainty without conscious report. In this study, we take inspiration from perceptual

55 decision-making studies, which have demonstrated that people implicitly incorporate uncertainty to increase behav-
56 ioral performance in a variety of decision-making paradigms (e.g., van Beers, Sittig, & Gon, 1999; Ernst & Banks,
57 2002; Alais & Burr, 2004; Körding & Wolpert, 2004; Knill & Pouget, 2004; Ma, Navalpakkam, Beck, van den Berg,
58 & Pouget, 2011; Jazayeri & Shadlen, 2010; Stocker & Simoncelli, 2006).

59 There is already some evidence that people use uncertainty implicitly in working memory-based decisions. Kesh-
60 vari and colleagues had humans complete a four-item orientation change detection task (Keshvari, van den Berg, &
61 Ma, 2012); Devkar and colleagues had humans and monkeys complete a three-item orientation change localization
62 task (Devkar, Wright, & Ma, 2017). Stimuli in both studies were ellipses, which were independently assigned to
63 be longer and narrower, providing “high-reliability” orientation information, or shorter and wider, providing “low-
64 reliability” orientation information. The reliability of ellipses affected the precision with which they were encoded,
65 and thus should have affected the memory uncertainty associated with each item. To maximize performance in both
66 tasks, participants’ uncertainty would need to reflect this variability in item-specific precision. Both studies found that
67 a computational model that assumes participants use item-specific uncertainty accounted better for people’s choices
68 than alternative models.

69 Crucially, while these two studies provide evidence that people can implicitly use uncertainty, some experimental
70 design choices do not allow us to conclude that people are actually maintaining uncertainty per se. First, participants
71 in the study by Devkar and colleagues received trial-to-trial feedback on the correctness of their response. It is thus
72 possible that participants simply learned a stimulus-response mapping (Maloney & Mamassian, 2009) rather than per-
73 forming Bayesian inference or other forms of probabilistic computation (i.e., still using uncertainty in their decision;
74 Ma, 2010). Second, precision in both studies was experimentally manipulated through ellipse reliability, which was
75 held constant through and available after the working memory delay. Thus, participants could have used this ellipse
76 reliability as a proxy for uncertainty (Barthelmé & Mamassian, 2010), rather than maintaining this information over
77 the working memory delay.

78 Thus, the goal of this study was to investigate the conjunction of uncertainty *maintenance* and *implicit use* in a
79 working memory task. To reach this goal, we collected data in a two-condition orientation change detection task and
80 developed computational models to test different hypotheses about uncertainty. Intuitively, uncertainty results in a
81 criterion shift, such that a stimulus with higher uncertainty associated with it would require a larger physical change
82 before an observer would report that it changed. In the first condition, we established that people use uncertainty if a
83 proxy to it is provided to them at the time of decision, replicating the results from Keshvari and others (2012). In the
84 second condition, we asked if people still use uncertainty if this proxy is not provided at the time of decision. In other
85 words, we asked if uncertainty is being maintained in working memory.

86 **3 Experimental Methods**

87 **3.1 Participants**

88 Thirteen participants (11 female; mean age $M = 21.1$ years, $SD = 2.5$) completed both conditions. All participants had
89 normal or corrected-to-normal vision. Participants were naive to the study's hypotheses and were paid \$12/hour and
90 a \$24 completion bonus. We obtained informed, written consent from all participants. The study was in accordance
91 with the Declaration of Helsinki and was approved by the Institutional Review Board of New York University (IRB-
92 FY2019-2490). Seven other participants were excluded because they did not meet performance criteria (explained in
93 the Cross-Session Procedure section).

94 **3.2 Stimuli**

95 Stimuli were four, light-grey, oriented ellipses on a medium-grey background. Each ellipse could be long or short, to
96 provide respectively higher or lower reliability information regarding the orientation of the ellipses. All ellipses had
97 an area of 1.19 degrees of visual angle (dva). The high-reliability ellipse had an ellipse eccentricity of 0.9, such that
98 the major and minor axis were 1.02 and 0.37 dva, respectively. The low-reliability ellipse eccentricity was determined
99 separately for each participant to equate performance (details in Procedure).

100 On every trial, a stimulus display consisted of four ellipses. The probability of each ellipse being high reliability
101 was 0.5, independent of the reliability of the other ellipses. The location of the first ellipse was drawn from a uniform
102 distribution between polar angles 0° and 90° . Each ellipse after that was placed such that all ellipses were 90° apart
103 on an imaginary annulus that was 7 dva away from fixation. Afterward, the x- and y- location of the ellipses were
104 independently jittered -0.3 to 0.3 dva. The ellipse stimuli are consistent to those in Keshavri et al.'s (2012) study. In
105 one condition, there were additionally oriented line stimuli, which were set to have approximately the same area as
106 the ellipses. Stimuli were displayed on a 23 inch LED monitor with a refresh rate of 60 Hz and a resolution of 1920 x
107 1080 pixels.

108 **3.3 Procedure**

109 **3.3.1 Trial Procedure**

110 **Ellipse condition.** A trial began with a fixation cross presented for 1000 ms. Four ellipses were presented for 100 ms,
111 followed by a 1000 ms delay, then by another four ellipses for 100 ms. On half of the trials, all ellipses in the second
112 stimulus presentation were identical to the ellipses in the first stimulus presentation. On the other half of the trials, one
113 ellipse changed in orientation. This change was drawn from a uniform distribution, so change of any magnitude had
114 equal probability. Each ellipse had an equal probability of containing the change. *Change* and *no change* trials were
115 randomly interleaved throughout the experiment. The participant indicated with a keyboard button press whether they
116 believed there was an orientation change between the two displays. This condition is identical to the experiment done
117 by Keshvari et al. (2012).

118 **Line condition.** In the Line condition, the stimuli in the second presentation were oriented lines rather than
119 ellipses. The task was otherwise identical. An example of a trial in the Ellipse and Line conditions is illustrated in
120 Figure 1.

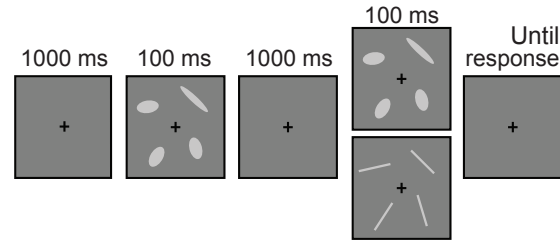


Figure 1: **Trial sequence.** Participants fixated on a cross, saw four ellipses (here showing one high-reliability ellipse and three low-reliability ellipses), maintained them over a delay, saw four stimuli again, and reported whether they believed there was an orientation change or not. In the Ellipse condition, ellipses in the second presentation were of the same reliability as in the first. In the Line condition, lines replaced ellipses in the second stimulus presentation, to avoid providing cues to the precision with which the first items were maintained.

121 3.3.2 Cross-Session Procedure

122 Participants completed both conditions over six one-hour sessions. They began their first session with a Practice
123 block, designed to ease the participants into the task. They then completed 2000 trials of each condition, preceded
124 by a Threshold block to set the “short” ellipse reliability for each condition. Participants completed all of one con-
125 dition before completing the other, and the order was counterbalanced across participants. Participants were verbally
126 informed that each trial had a 0.5 probability of a change occurring, that a change (if present) would occur in exactly
127 one ellipse, and the change could be “of any magnitude; big changes are as possible as small changes.” Participants
128 were also verbally informed that some ellipses would be more elongated than others, that this may affect performance,
129 and that half of the experiment would involve the stimuli changing from ellipses to lines. They were informed that
130 their task did not change; the goal was always to indicate whether there was a change in orientation.

131 The Practice block consisted of 256 trials and was designed to ease naive participants into the speed of the task.
132 The stimulus presentation time decreased throughout the course of the Practice block, from 333 ms to 100 ms, in 33
133 ms increments every 32 trials. Unlike the actual task, the ellipse eccentricities (i.e., reliabilities) of all ellipses within
134 each trial were the same, but changed across trials. The stimuli in the second stimulus presentation corresponded to
135 the condition that the participant completed first. For example, the stimuli in the second presentation were lines if the
136 participant completed the Line condition first.

137 The Threshold block consisted of 400 trials and was used to set the ellipse eccentricity of the low-reliability ellipse
138 in each condition. Like the Practice block, the ellipse eccentricities of all ellipses on each trial were the same, but
139 changed on a trial-to-trial basis. The second stimulus presentation set were either ellipses or lines, corresponding to
140 which condition the threshold was being set for. A cumulative normal psychometric function was fit to the accuracy as

141 a function of ellipse eccentricity, and the low-reliability ellipse eccentricity was set as the value that corresponded to a
 142 predicted 65% accuracy. If the ceiling performance of the participant was estimated to be less than 75%, the Threshold
 143 block was repeated. If the psychometric function could not estimate an ellipse reliability for which performance would
 144 hit 65% after the second try, the participant was excluded from the experiment. Seven participants were excluded based
 145 on these criteria.

146 4 Experimental Results

147 The goal of our study was to investigate whether people maintained and used uncertainty implicitly in a working
 148 memory-based decision. To do this, we conducted a two-condition orientation change detection task. People could use
 149 memory uncertainty to maximize performance in both conditions, but only the Line condition required maintenance of
 150 that uncertainty. We conducted five repeated-measures ANOVAs to test whether condition (Ellipse, Line), the number
 151 of high-reliability ellipses displayed (N_{high} : 0, 1, 2, 3, 4), or their interaction significantly affected the following
 152 values: proportion report “change,” false alarm rate, hit rate (for all items), hit rate (when the changed item was a
 153 low-reliability ellipse), and hit rate (when the changed item was a high-reliability ellipse). These values are visualized
 154 in Figure 2, and the statistics are reported in Table 1.

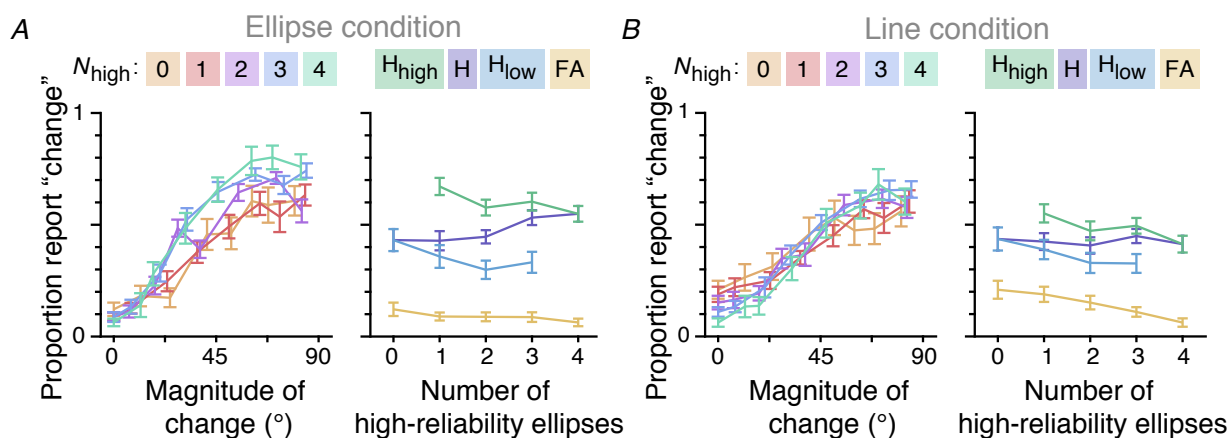


Figure 2: **Behavioral data.** Illustration of behavioral data for (A) Ellipse condition and (B) Line condition. For each condition, the left plots illustrate proportion report “change” as a function of magnitude of change. Data are binned by quantile, and different colored lines illustrate data from trials with different numbers of high-reliability ellipses presented on the first display. The right plots illustrate the proportion report “change” as a function of number of high-reliability ellipses, conditioned on whether there was no actual change (false alarm (FA): yellow), a change in a low-reliability ellipse (H_{low} : blue), a change in a high-reliability ellipse (H_{high} : green), or a change in any ellipse (hit (H): purple). Color legends are displayed above the plots. Note that the aggregated hits are a weighted combination of the reliability-conditioned hits. The “Z” shape formed by the hit lines are an instance of Simpson’s paradox.

Dependent variable	Factor	Statistics	p	ϵ	η^2
Proportion report “change”	N_{high}	$F(1.38, 16.50) = 3.37$	0.07	0.34	0.03
	Condition	$F(1, 12) = 1.33$	0.27	–	0.01
	N_{high} x condition	$F(2.12, 25.38) = 6.32$	0.005	0.52	0.04
False alarm rate	N_{high}	$F(1.93, 23.17) = 18.21$	2.07×10^{-5}	0.48	0.14
	Condition	$F(1, 12) = 6.50$	0.03	–	0.08
	N_{high} x condition	$F(1.95, 23.36) = 4.94$	0.02	0.49	0.05
Hit rate (all)	N_{high}	$F(1.36, 16.30) = 5.29$	0.03	0.34	0.04
	Condition	$F(1, 12) = 2.47$	0.14	–	0.03
	N_{high} x condition	$F(2.04, 24.48) = 5.33$	0.01	0.51	0.03
Hit rate (low-reliability)	N_{high}	$F(1.76, 21.07) = 23.26$	8.43×10^{-6}	0.59	0.08
	Condition	$F(1, 12) = 0.29$	0.60	–	0.005
	N_{high} x condition	$F(2.01, 24.15) = 0.37$	0.69	0.67	0.002
Hit rate (high-reliability)	N_{high}	$F(1.98, 23.79) = 35.44$	7.72×10^{-8}	0.66	0.13
	Condition	$F(1, 12) = 14.66$	0.002	–	0.17
	N_{high} x condition	$F(2.15, 25.80) = 0.75$	0.49	0.72	0.003

Table 1: **Results of two-way repeated-measures ANOVA.** Independent variables are N_{high} (0,1,2,3,4) and condition (Ellipse, Line), and dependent variables are displayed as the first column. Statistics of significant effects are bolded. For all ANOVAs, we report the Greenhouse-Geisser corrected results and ϵ (sphericity correction) when appropriate.

155 There was a statistically significant interaction between N_{high} and condition on proportion report “change.” In only
156 the Ellipse condition, the proportion report “change” was modulated by the number of high-reliability ellipses (left
157 plot of Fig. 2 A, B). There were significantly more false alarms in the Line condition ($M = 0.14$, $SEM = 0.03$) than
158 in the Ellipse condition ($M = 0.09$, $SEM = 0.02$; yellow lines in right plots of Fig. 2 A, B). Perhaps people confused
159 changes in stimuli as changes in orientation.

160 Both reliability-conditioned hit rates (blue and green lines in right plots of Fig. 2 A, B) as well as false alarm
161 rates decreased with increasing N_{high} . Additionally, participants had significantly lower high-reliability hits in the Line
162 condition and the Ellipse condition. These results could be potentially explained by participants using uncertainty
163 information. As the total number of high-reliability ellipses, N_{high} , increases, the number of high-reliability ellipses
164 that do not change also increases. If people weigh high-reliability information more heavily than low-reliability infor-
165 mation, then as the amount of high-reliability “no change” information increases, the proportion that the participants
166 respond “change” should decrease. This would result in a decrease in reliability-conditioned hit rates and false alarm
167 rates with increasing N_{high} .

168 There is an interesting reverse in the qualitative trend when looking at all hit rates across all trials: hit rate increases
169 as a function of N_{high} . This Simpson’s paradox is a result of weighted averaging and the performance difference

170 between the reliability-conditioned hit rates. As the number of high-reliability ellipses in a display increases, so does
171 the probability of a change occurring in a high-reliability ellipse. Thus, the total hit rates for higher N_{high} s contain
172 more high-reliability hits than low-reliability hits, driving this value upward. Similarly, the trials to compute hit rates
173 for lower N_{high} s predominantly contain changes in low-reliability ellipses, thus driving the average downward. There
174 was also a significant effect of condition; hit rates were higher in the Ellipse condition.

175 These statistics show that differences between factors and conditions exist, but are dissatisfying because they do
176 not offer explanations of what these differences mean. In fact, the intuitions presented in this section are largely driven
177 by knowledge about how noise affects decisions, knowledge acquired from computational models like signal detection
178 theory (e.g., Green & Swets, 1966) and Bayesian decision theory. Thus, in this paper we directly test our intuitions
179 about the underlying working memory processes through computational modeling. Computational modeling allows
180 us to make explicit assumptions and precise quantitative predictions, which provide committal, falsifiable explanations
181 of the processes involved.

182 **5 Modeling Methods**

183 To test whether people are maintaining and using uncertainty when making their change detection decision, we use
184 Bayesian observer models (Ma, 2019). Bayesian models provide a normative, flexible, and interpretable framework
185 to study the working memory process. These models are particularly useful in cases where the observer is trying
186 to make a decision without full knowledge of task-relevant information. In working memory, people do not have
187 full knowledge because information is not remembered perfectly. While Bayesian decision theory describes how an
188 observer should behave in order to maximize performance, different components of the model can be easily substituted
189 with incorrect beliefs or suboptimal use of information, and thus provides a good template for building models with
190 “imperfectly optimal observers” (Maloney & Zhang, 2010) or “model mismatch” (Orhan & Jacobs, 2014; Beck, Ma,
191 Pitkow, Latham, & Pouget, 2012; Acerbi, Vijayakumar, & Wolpert, 2014).

192 We model the observer’s decision process as consisting of an encoding stage and a decision stage. The encoding
193 stage describes the task statistics and our assumptions about how memories are generated. In the decision stage, the ob-
194 server calculates a decision variable based on their belief of the encoding stage and decides whether to report “change”
195 or “no change” based on some decision rule. We compared two models: one in which uncertainty is maintained and
196 used and another that is not, named the “Use Uncertainty” and the “Ignore Uncertainty” model, respectively. This
197 section describes how these models were defined, fit, and compared.

198 **5.1 Encoding Stage**

199 In this section, we define the statistical structure of the experiment and define our assumptions about how memories
200 are generated in an observer. On every trial, there is a 0.5 probability of there being a change, $p(C = 1) = 0.5$, where C
201 takes values 0 (no change) and 1 (change). On change trials, exactly one item changes in its orientation, and each item
202 is equally probable to be changed. The orientation change, Δ , is drawn from a uniform distribution, $p(\Delta) = \frac{1}{2\pi}$. (For

203 mathematical convenience, and without loss of generality, we doubled the actual orientation of stimuli in all model
 204 specifications such that the values span 0 to 2π rather than 0 to π . We do not double these values when illustrating
 205 model fits.)

206 We denote the vector of all orientations of the items presented on the first display by ξ , in which each element is an
 207 independent draw from a uniform distribution over orientation space. The vector of orientations at the second display,
 208 ϕ , was identical to ξ in no change trials. In change trials, the i th element of ϕ , the location of change, was equivalent
 209 to $\xi_i + \Delta$.

210 We model the memory process for each item of each display according to the Variable Precision model (van den
 211 Berg et al., 2012; Fougne et al., 2012), by which memories are described as a continuous resource that randomly
 212 fluctuates across items and trials. The noisy measurements of each item on each display, $\mathbf{x} = (x_1, \dots, x_N)$ and $\mathbf{y} =$
 213 (y_1, \dots, y_N) , are conditionally independent and drawn from a Von Mises distribution centered on the actual orientation
 214 presentation,

$$p(\mathbf{x}|\xi; \kappa_x) = \prod_{i=1}^N p(x_i|\xi_i, \kappa_{x,i}) = \prod_{i=1}^N \frac{1}{2\pi I_0(\kappa_{x,i})} e^{\kappa_{x,i} \cos(x_i - \xi_i)}$$

$$p(\mathbf{y}|\phi; \kappa_y) = \prod_{i=1}^N p(y_i|\phi_i, \kappa_{y,i}) = \prod_{i=1}^N \frac{1}{2\pi I_0(\kappa_{y,i})} e^{\kappa_{y,i} \cos(y_i - \phi_i)}.$$

215 The κ s are the concentration parameter of the Von Mises distribution, and are related to the precision with which each
 216 item is remembered; a higher κ corresponds to higher precision. The subscript of each κ indicates which item it refers
 217 to (e.g., $\kappa_{x,i}$ is concentration parameter for x_i , the i th item the first stimulus presentation). We assume that memory
 218 precision varies across items, above and beyond the precision differences due to stimulus reliability. In other words,
 219 $\kappa_{x,i}$ and $\kappa_{y,i}$ are themselves random variables, rather than single values. Rather than sampling κ itself, we sample the
 220 Fisher information of the Von Mises distribution, J , from a gamma distribution:

$$p(J) = \frac{1}{\Gamma\left(\frac{\bar{J}}{\tau}\right) \tau^{\bar{J}/\tau}} J^{\bar{J}/\tau - 1} e^{-J/\tau},$$

221 where τ is the scale parameter of the gamma distribution and \bar{J} is the mean precision. The relationship between J and
 222 κ is the following:

$$J = \kappa \frac{I_1(\kappa)}{I_0(\kappa)},$$

223 where I_0 is a modified Bessel function of the first kind of order 0 and I_1 is a modified Bessel function of the first kind
 224 of order 1 (van den Berg et al., 2012; Keshvari et al., 2012). We allow the mean precision to differ across stimulus
 225 shape; the precisions of memories corresponding to low-reliability ellipses are drawn from a gamma distribution with
 226 mean \bar{J}_{low} and high-reliability ellipses with mean \bar{J}_{high} . Parameter τ is shared across both distributions. Because items
 227 in the first display were presented earlier, there are certainly differences in the precision with which items in the first
 228 and second display are maintained, independent of ellipse reliability. However, the amount that the first and second
 229 displays contribute to the overall measured change are extremely hard to tease apart in the model. Thus, we use one
 230 parameter per reliability and recognize that this estimate will be some average of the precisions of the first and second
 231 display.

232 When modeling the Line condition, we have an additional parameter, \bar{J}_{line} , which corresponds to the mean precision
 233 with which each line on the second display is remembered by the observer. To limit model complexity, the gamma
 234 function from which each line’s precision is drawn shares the same scale parameter τ as the distributions from which
 235 the ellipse precisions are drawn.

236 5.2 Decoding Stage

237 5.2.1 Decision Variable

238 The essence of Bayesian inference is that an observer can compute a posterior over task-relevant latent variables, and
 239 should if they want to maximize performance. In this case, the observer should calculate the probability of the state
 240 of the world (i.e., change or no change) given their observations, $p(C|\mathbf{x}, \mathbf{y})$, which they can compute using Bayes rule.
 241 With a scenario in which there are only two states of the world, it is convenient to combine these into a ratio. Thus,
 242 we assume the observer calculates, for each item, the ratio of the likelihood of there being change and the likelihood
 243 of there being no change:

$$d = \frac{p(C = 1|\mathbf{x}, \mathbf{y})}{p(C = 0|\mathbf{x}, \mathbf{y})} = \frac{p(\mathbf{x}, \mathbf{y}|C = 1)p(C = 1)}{p(\mathbf{x}, \mathbf{y}|C = 0)p(C = 0)}. \quad (1)$$

244 Details of the derivation can be found in Appendix 8.1, but this simplifies to the following expression:

$$d = \frac{p(C = 1)}{p(C = 0)} \frac{1}{N} \sum_{i=1}^N d_i, \quad (2)$$

245 where

$$d_i = \frac{I_0(\kappa_{x,i})I_0(\kappa_{y,i})}{I_0\left(\sqrt{\kappa_{x,i}^2 + \kappa_{y,i}^2 + 2\kappa_{x,i}\kappa_{y,i}\cos(x_i - y_i)}\right)}. \quad (3)$$

246 I_0 is a modified Bessel function of the first kind of order 0, and the κ s are the concentration parameters of the noise
 247 distributions for the item indicated in the subscript. Intuitively, d_i provides a measure of the evidence of change for the
 248 i^{th} item. It increases with the measured amount of change, $x_i - y_i$, weighted by a function of the precisions with which
 249 x_i and y_i are remembered. The d_i s are averaged in the decision variable d , providing the optimal measure of evidence
 250 of change of the entire display.

251 This is the step in which the use of uncertainty comes in. Observers who correctly maintain and use uncertainty
 252 (i.e., observers who act in accordance with the optimal, “Use Uncertainty” model) compute d_i exactly as described.
 253 However, observers acting in accordance with the “Ignore Uncertainty” model do not know or do not consider that
 254 the precision of their memories for all items in both displays varies. Computing the decision rule for the Ignore
 255 Uncertainty observer is the same as replacing all κ s in Eq. 3 with a constant, resulting in the following local decision
 256 variable:

$$d_i = \frac{I_0^2(\kappa_{\text{ass}})}{I_0\left(\kappa_{\text{ass}}\sqrt{2 + 2\cos(x_i - y_i)}\right)}, \quad (4)$$

257 where κ_{ass} is the assumed precision for all items on all displays. The decision variable thus becomes just a function
258 of $\cos(x_i - y_i)$, because the remainder of the expression is constant. The Ignore Uncertainty observer thus ignores any
259 factor that could have affected their memory precision. We recognize this is a strong assumption, and we weaken it in
260 the subsequent Model Variants section.

261 5.2.2 Decision Rule

262 The observer maps this decision variable onto a response by reporting “change” whenever the probability of there
263 being a change is greater than 0.5 (Figure 3). An optimal observer would thus report “change” when the ratio of
264 the likelihood of there being a change and the likelihood of there being no change (Eq. 2) is greater than 1. For
265 convenience, we use the logarithm of the likelihood ratio; the optimal observer would thus report “change” if this
266 value is greater than 0. However, we allow the observer to have some response bias (e.g., due to unequal priors,
267 rewards, or motor costs), and thus implement the following decision rule:

$$\log \left(\frac{1}{N} \sum_{i=1}^N d_i \right) > k, \quad (5)$$

268 where k is a free parameter. For both models, we implemented global decision noise by adding zero-mean Gaussian
269 noise with standard deviation σ_d to the log of decision variable d (Keshvari et al., 2012; Acerbi et al., 2014; Mueller
270 & Weidemann, 2008). Additionally, participants randomly guess with probability λ , due to factors such as lapses in
271 attention.

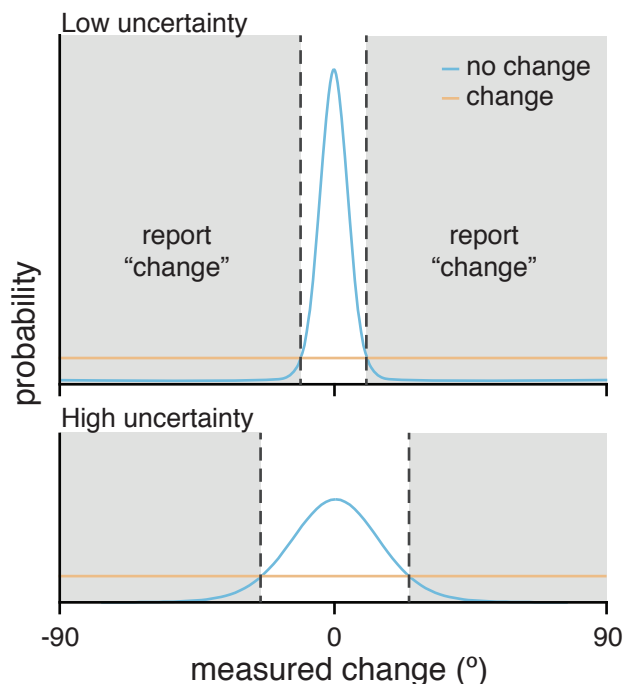


Figure 3: **Model didactics.** This didactic illustrates a simplified one-item version of this task. The probability of the measured change for an item given that the item did (orange) or did not (blue) change orientation, as estimated by the optimal observer. Uncertainty modulates the width of the no change distribution, such that higher uncertainty makes the no change distribution wider (bottom). The optimal observer (with $k = 0$) places their decision boundaries at the intersection of the change and no change distributions (vertical dashed lines), reporting “change” whenever that state of the world is more probable (shaded region) and “no change” otherwise.

272 5.3 Parameter Estimation and Model Comparison

273 5.3.1 Parameters

274 Both models in both conditions have parameters \bar{J}_{high} , \bar{J}_{low} , τ , k , λ , and σ_d . Parameters \bar{J}_{high} and \bar{J}_{low} correspond to the
 275 mean precision of the high- and low-reliability ellipses, respectively. Precision is also affected by the scale parameter
 276 of the gamma distribution from which item-wise precision is drawn, τ ; this value is shared across the two ellipse types
 277 and the line when applicable. Parameter k is the observer’s response bias; λ is the probability on each trial that the
 278 observer lapses and responds randomly; σ_d is the standard deviation of the Gaussian from which decision noise is
 279 simulated.

280 When fitting data from the Line condition, there is an additional parameter \bar{J}_{line} , corresponding to the mean preci-
 281 sion with which the line stimulus is represented. The Ignore Uncertainty model has one additional parameter: J_{ass} , the
 282 assumed precision of all stimuli in both displays.

283 5.3.2 Parameter Estimation

284 The likelihood of the parameter combination θ for a given participant and model is the probability of the data given
285 the parameter combination. We used the log likelihood, which we denote LL:

$$\begin{aligned} \text{LL}(\theta) &= \log p(\theta | \text{data, model}) \\ &= \log \prod_t^{N_{\text{trials}}} p(r_t | \theta) \\ &= \sum_t^{N_{\text{trials}}} \log p(r_t | \theta), \end{aligned}$$

286 where r_t is the participant's response on the t^{th} trial. For each participant, we used maximum-likelihood estimation to
287 find which parameter combination best describes participant's data. Computing the LL analytically is intractable, so
288 we used Inverse Binomial Sampling (IBS; van Opheusden, Acerbi, & Ma, 2020), a method which efficiently computes
289 an unbiased estimate of the LL. This calculation is stochastic, so we additionally used an optimization algorithm that
290 can account for stochasticity and expensive LL evaluations (BADS; Acerbi & Ma, 2017). BADS explicitly incorpo-
291 rates uncertainty in the estimated LL and converges in fewer function evaluations than other stochastic optimization
292 methods (e.g., CMA-ES, genetic algorithms), making it an ideal optimization method when likelihood calculations are
293 computationally expensive and stochastic. We used 20 different starting positions, using Latin hypercube sampling, to
294 reduce the probability of finding a local minimum. We took the parameter combination corresponding to the minimum
295 negative log-likelihood of our runs as the ML parameter estimate. The estimated LL at the candidate optimum was
296 reevaluated using 1000 repetitions in IBS, in order to reduce the standard deviation of estimation noise to less than 1.
297 We denote the maximum log-likelihood by LL^* .

298 5.3.3 Model Comparison

We compared models using corrected Akaike Information Criterion (AICc; Hurvich & Tsai, 1987) and the Bayesian
Information Criterion (BIC; Schwarz, 1978). BIC penalizes for number of model parameters N_{pars} harsher than AICc
does.

$$\begin{aligned} \text{AICc} &= -2\text{LL}^* + 2N_{\text{pars}} + \frac{2N_{\text{pars}}(N_{\text{pars}} + 1)}{N_{\text{trials}} - N_{\text{pars}} - 1} \\ \text{BIC} &= -2\text{LL}^* + 2N_{\text{pars}} \log N_{\text{trials}} \end{aligned}$$

299 5.4 Modeling Results

300 We compared the fits of the Use Uncertainty and Ignore Uncertainty models to each of the conditions separately. The
301 Use Uncertainty model provides a good qualitative fit to the data in both conditions (top row of Figure 4A), while the
302 Ignore Uncertainty model is unable to capture the data (bottom row of Figure 4A). To compare models quantitatively,
303 we used summed ΔAICc and ΔBIC , that is the difference of summed AICc (resp. BIC) across participants between
304 the Ignore Uncertainty and Use Uncertainty models (positive values mean that Use Uncertainty fits better). Summing

305 model comparison metrics across participants implicitly assumes that all participants are fit by the same model. For
306 both conditions and model comparison metrics, participants were better fit by the Use Uncertainty model than the
307 Ignore Uncertainty model (summed [95% bootstrapped confidence interval (CI)] Δ AICc across subjects – Ellipse:
308 3091 [2015, 4321], Line: 2764 [1468, 4400]. Δ BIC – Ellipse: 3263 [2155, 4450], Line: 2935 [1640, 4433]). Note
309 that, while reporting the summed Δ AICc and Δ BIC, for visualization we plot the individual differences and plot the
310 95% CIs of the median Δ AICc (Figure 4B). Parameter estimates for the Use Uncertainty model in the Ellipse and Line
311 condition can be found in the Appendix (Tables 4 and 5, respectively).

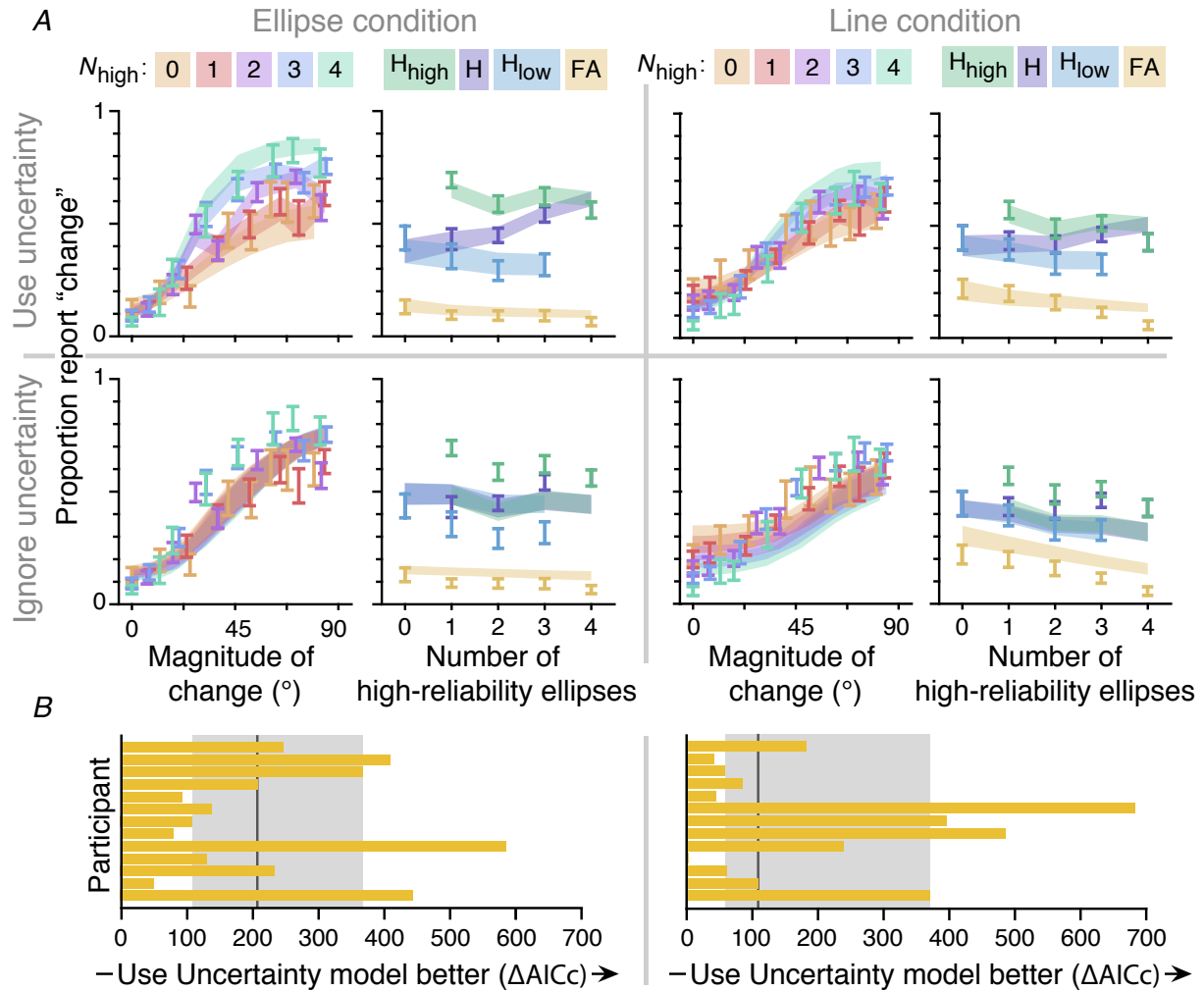


Figure 4: **Model fits.** *A.* $M \pm SEM$ data (error bars) and model fits (fills) for the Use (top) and Ignore (bottom) Uncertainty models and the Ellipse (left) and Line (right) conditions. For each model and condition, the left graph illustrates the proportion report “change” as a function of amount of change. Data and models are binned by quantiles, and color indicates the number of high-reliability ellipses in the first display. The right graph illustrates the proportion hits for high-reliability items (green), hits for low-reliability items (blue), total hits (purple), and false alarms (yellow) as a function of number of high-reliability items. *B.* Model comparison for the Ellipse (left) and Line (right) conditions. Each bar indicates the individual-subject ΔAICc between the Use and Ignore Uncertainty models, where a positive value indicates that the Use Uncertainty model is favored. The vertical grey line indicates the median across participants, and the shaded region illustrates the 95% bootstrapped confidence interval of the median. Only ΔAICc s are illustrated here; ΔBIC s gave similar results.

312 **6 Model Variants**

313 While the Use Uncertainty model provides a good fit to the data, the two models we have considered thus far contain
314 strong assumptions that uncertainty is either perfectly used or entirely ignored. In this section, we modify the as-
315 sumptions by factorially comparing different formulations of the encoding, inference, and decision stage of the model
316 (van den Berg, Awh, & Ma, 2014; Acerbi, Wolpert, & Vijayakumar, 2012; Keshvari et al., 2012). A factorial model
317 comparison is an effective way of testing which of the assumptions we made were critical for accounting for human
318 behavior, and thus which are reasonable to make conclusions about. In this section, we demonstrate that our general
319 conclusions about the use of uncertainty do not depend on the specific assumptions we made when defining our model.
320 We only discuss the results of the Line condition here, since it is the only condition that investigates the maintenance of
321 uncertainty in working memory. However, we did the same analysis to the Ellipse condition data and found consistent
322 results (Appendix 8.3).

323 **6.1 Encoding**

324 In both the Use and Ignore Uncertainty models, we assumed that observers' encoding noise followed that of a Variable
325 Precision model (van den Berg et al., 2012; Fougny et al., 2012). Here, we also consider that observers' memory pre-
326 cision varies only based on stimulus type, and does not fluctuate on an item-to-item basis. With this "Fixed Precision"
327 assumption of encoding noise, the κ for each item is determined only by its stimulus type; high-reliability ellipses
328 would be encoded with parameter κ_{high} , low-reliability ellipses with κ_{low} , and lines with κ_{line} .

329 **6.2 Inference**

330 Observers calculate the decision variable according to some inference process, which we allow to be independent of
331 the true generative process. The potential model mismatch (Orhan & Jacobs, 2014; Beck et al., 2012; Acerbi et al.,
332 2014) between the true and believed generative process could be due to a result of wrong beliefs about the generative
333 process or computation limitations that prevent accurate representation of the generative model. We consider that
334 observers may use partial knowledge of uncertainty, rather than fully Using or Ignoring uncertainty.

335 We consider that the observer may have one of four inference models, listed below in decreasing order of how
336 many factors the observer takes into account in their uncertainty:

- 337 1. Variable precision (V): the observer believes that mean memory precision varies with the exact stimulus shape
338 (low-reliability ellipse, high-reliability ellipse, line) and that there is additional noise for each item at each
339 presentation. This inference model is optimal when the true generative process is Variable precision.
- 340 2. Fixed precision (F): the observer believes that memory precision varies with the exact stimulus shape (low-
341 reliability ellipse, high-reliability ellipse, line), but does not consider that there is additional noise for each item
342 at each presentation. This inference model is suboptimal when the true generative process is Variable precision,
343 but optimal when the true generative process is Fixed precision.

344 3. Limited (L): the observer believes that memory precision varies across shapes (ellipse vs. line). This observer
345 does not consider differences in precision between high- and low-reliability ellipses or additional noise for each
346 item at each presentation. This observer is suboptimal.

347 4. Same precision (S): the observer believes that memory precision is the same throughout the condition, and does
348 not vary with stimulus shape or anything else. This is the “Ignore Uncertainty” observer and is suboptimal.

349 Note that the Variable and Same precision inference schemes here are identical to that of Keshvari and others’ (2012),
350 and the Fixed precision here is equivalent to their “Equal” precision inference scheme.

351 **6.3 Decision Rule**

352 The Use and Ignore Uncertainty models use the optimal decision rule (Eq. 5). Note that participants may have
353 incorrect assumptions about the noise in their memory, but still be acting in accordance with Bayesian decision theory
354 (i.e., still using the correct decision rule), resulting in “imperfectly optimal observers” (Maloney & Zhang, 2010).
355 Alternatively, participants could be calculating the optimal decision variable, but be using a suboptimal decision rule.
356 Here, we consider observers who use the max rule, reporting “change” whenever the maximum evidence of change is
357 greater than some criterion, k ,

$$\max_i d_i > k, \quad (6)$$

358 rather than averaging d_i s. These observers are not Bayes-optimal, but are still using probabilistic computation (i.e., still
359 using their uncertainty) in the calculation of d_i . In fact, in many cases these decision rules do not result in substantially
360 different behavior (Ma, Shen, Dziugaite, & van den Berg, 2015). For example, if all d_i s are similar, then a max and an
361 average will result in similar values. If the maximum d_i is substantially larger than the others, both decision rules can
362 result in similar behavior by adjusting k .

363 **6.4 Parameters**

364 There are two possible encoding schemes ((V)ariable, (F)ixed), four possible inference schemes ((V)ariable, (F)ixed,
365 (L)imited, (S)ame), and two possible decision rules ((O)ptimal, (M)ax). Factorially combining each of these char-
366 acteristics would yield 16 different models. We choose not to consider the models in which the generative model is
367 “F” but the observer assumes “V” under the assumption that people tend not to assume the (perceptual) world is more
368 complicated than it actually is; thus, we test a total of 14 models. We denote each model by the letters corresponding to
369 their encoding scheme, inference scheme, and decision rule (e.g., VVO is the model with Variable precision encoding,
370 an observer assumes Variable precision, and an Optimal decision rule). The VVO model is the Use Uncertainty model;
371 the VSO model is the Ignore Uncertainty model.

372 *Encoding parameters.* Like before, observers with Variable precision encoding have parameters \bar{J}_{high} , \bar{J}_{low} , \bar{J}_{line} ,
373 and τ . Observers with Fixed precision encoding have parameters J_{high} , J_{low} , and J_{line} .

374 *Inference parameters.* For the observer who correctly infers their encoding process (i.e., VVO, VVM, FFO, or
 375 FFM), there are no additional parameters. If the observer has Variable precision encoding but does not take into account
 376 individual-item variations (i.e., VFO or VFM), then the assumed precision is $J_{\text{high}} = \bar{J}_{\text{high}}$, $J_{\text{low}} = \bar{J}_{\text{low}}$, and $J_{\text{line}} = \bar{J}_{\text{line}}$
 377 for high-reliability ellipses, low-reliability ellipses, and lines, respectively. Limited inference observers (i.e., VLO,
 378 VLM, FLO, FLM) have two additional parameters: $J_{\text{ass},e}$ and $J_{\text{ass},l}$, corresponding to the assumed precision of the
 379 ellipses and lines, respectively. Same inference observers, who do not take any memory variations into account (i.e.,
 380 VSO, VSM, FSO, FSM), have one additional parameter J_{ass} , corresponding to the assumed precision of all items.

381 *Decision parameters.* Observers using both the optimal or max decision rule have parameter k , corresponding to
 382 the decision criterion. If any item has a decision variable greater than k , then they will report “change.”

383 Each model and their corresponding parameters is listed in Table 2. Note that the Same inference observer who
 384 uses the max rule (i.e., VSM, FSM) has one less parameter than their Optimal decision rule counterpart (i.e., VSO,
 385 FSO) because making a decision depends only on the item with the largest measured change.

Encoding	Inference	Decision Rule	
		(O)ptimal	(M)ax
(V)ariable	(V)ariable	$\bar{J}_{\text{high}}, \bar{J}_{\text{low}}, \tau, k, \lambda, \sigma_d(\bar{J}_{\text{line}})$	$\bar{J}_{\text{high}}, \bar{J}_{\text{low}}, \tau, k, \lambda, \sigma_d(\bar{J}_{\text{line}})$
	(F)ixed	$\bar{J}_{\text{high}}, \bar{J}_{\text{low}}, \tau, k, \lambda, \sigma_d(\bar{J}_{\text{line}})$	$\bar{J}_{\text{high}}, \bar{J}_{\text{low}}, \tau, k, \lambda, \sigma_d(\bar{J}_{\text{line}})$
	(L)imited	$\bar{J}_{\text{high}}, \bar{J}_{\text{low}}, \bar{J}_{\text{ass},e}, \tau, k, \lambda, \sigma_d(\bar{J}_{\text{line}}, \bar{J}_{\text{ass},l})$	$\bar{J}_{\text{high}}, \bar{J}_{\text{low}}, \bar{J}_{\text{ass},e}, \tau, k, \lambda, \sigma_d(\bar{J}_{\text{line}}, \bar{J}_{\text{ass},l})$
	(S)ame	$\bar{J}_{\text{high}}, \bar{J}_{\text{low}}, \bar{J}_{\text{ass}}, \tau, k, \lambda, \sigma_d(\bar{J}_{\text{line}})$	$\bar{J}_{\text{high}}, \bar{J}_{\text{low}}, \tau, k, \lambda, \sigma_d(\bar{J}_{\text{line}})$
(F)ixed	(F)ixed	$J_{\text{high}}, J_{\text{low}}, k, \lambda, \sigma_d(J_{\text{line}})$	$J_{\text{high}}, J_{\text{low}}, k, \lambda, \sigma_d(J_{\text{line}})$
	(L)imited	$J_{\text{high}}, J_{\text{low}}, J_{\text{ass},e}, k, \lambda, \sigma_d(J_{\text{line}}, J_{\text{ass},l})$	$J_{\text{high}}, J_{\text{low}}, J_{\text{ass},e}, k, \lambda, \sigma_d(J_{\text{line}}, J_{\text{ass},l})$
	(S)ame	$J_{\text{high}}, J_{\text{low}}, J_{\text{ass}}, k, \lambda, \sigma_d(J_{\text{line}})$	$J_{\text{high}}, J_{\text{low}}, k, \lambda, \sigma_d(J_{\text{line}})$

Table 2: **Model parameters.** Model parameters for Line condition. Parameters **not used** for fitting the Ellipse condition are displayed in parentheses. The top colored cell corresponds to parameters of the Use Uncertainty (VVO) model. The bottom colored cell corresponds to the parameters of the Ignore Uncertainty (VSO) model.

386 6.5 Model Comparison Results

387 6.5.1 Comparison of individual models

388 As previously described, we estimated parameters for each participant and compared models using AICc and BIC.
 389 In this section, we only discuss the results of the Line condition using summed AICc and BIC differences between
 390 the VVO (Use Uncertainty) and other models. We only discuss the data from the Line condition because it is the
 391 only condition that allows us to interrogate whether people are *maintaining* the uncertainty that they use in the change
 392 detection decision. For completeness, we report the results of the Ellipse condition in the Appendix 8.3.

393 When using AICc, the VVO model seems to be able to capture the human data the best, indicated by a positive
 394 summed ΔAICc and 95% bootstrapped CIs compared to all alternative models. When using ΔBIC , the VVO model

395 still fits best, but the 95% CIs are not above 0 for the FFO model, indicating that VVO does not fit the data significantly
 396 better than the FFO model. Qualitatively, both VVO and FFO models fit the data well (Figure 5). Note that, while
 397 reporting the summed ΔAICc and ΔBIC , we plot the individual differences and plot the 95% bootstrapped CIs of the
 398 median ΔAICc .

399 In the Appendix, we additionally report the results of group Bayesian Model Selection (BMS) for both condi-
 400 tions (Appendix 8.4). While summing the ΔAICc and ΔBIC implicitly assumes that participants are all fit by the
 401 same model, group BMS allows for participant heterogeneity and directly infers the distribution of participants across
 402 models. Using this alternative model comparison metric does not really change our results; VVO and FFO fit the par-
 403 ticipants' data substantially better than other models, but their performance against one another depend on the model
 404 comparison metric.

Encoding	Inference	Decision Rule			
		(O)ptimal		(M)ax	
		ΔAICc	ΔBIC	ΔAICc	ΔBIC
(V)ariable	(V)ariable	0 [0, 0]	0 [0, 0]	119 [19, 247]	119 [26, 247]
	(F)ixed	295 [119, 502]	295 [114, 477]	381 [201, 569]	381 [200, 578]
	(L)imited	2069 [957, 3433]	2411 [1326, 3766]	3167 [1667, 4688]	3510 [2212, 5220]
	(S)ame	2764 [1468, 4400]	2935 [1640, 4433]	2680 [1973, 3513]	2680 [1993, 3478]
(F)ixed	(F)ixed	480 [36, 1225]	309 [-141, 1018]	360 [218, 528]	188 [46, 345]
	(L)imited	1685 [541, 3130]	1857 [723, 3198]	1738 [558, 3277]	1909 [700, 3453]
	(S)ame	1098 [425, 1923]	1098 [379, 2038]	2220 [1487, 3150]	2049 [1337, 2976]

Table 3: **Summed ΔAICc and ΔBIC : Line condition.** The sum and 95% bootstrapped confidence interval of the AICc and BIC differences between the optimal VVO (Use Uncertainty) model and others. A positive value indicates that the VVO model provides a better fit to the data. The cells corresponding to the Use (VVO) and Ignore (VSO) Uncertainty models are colored in blue.

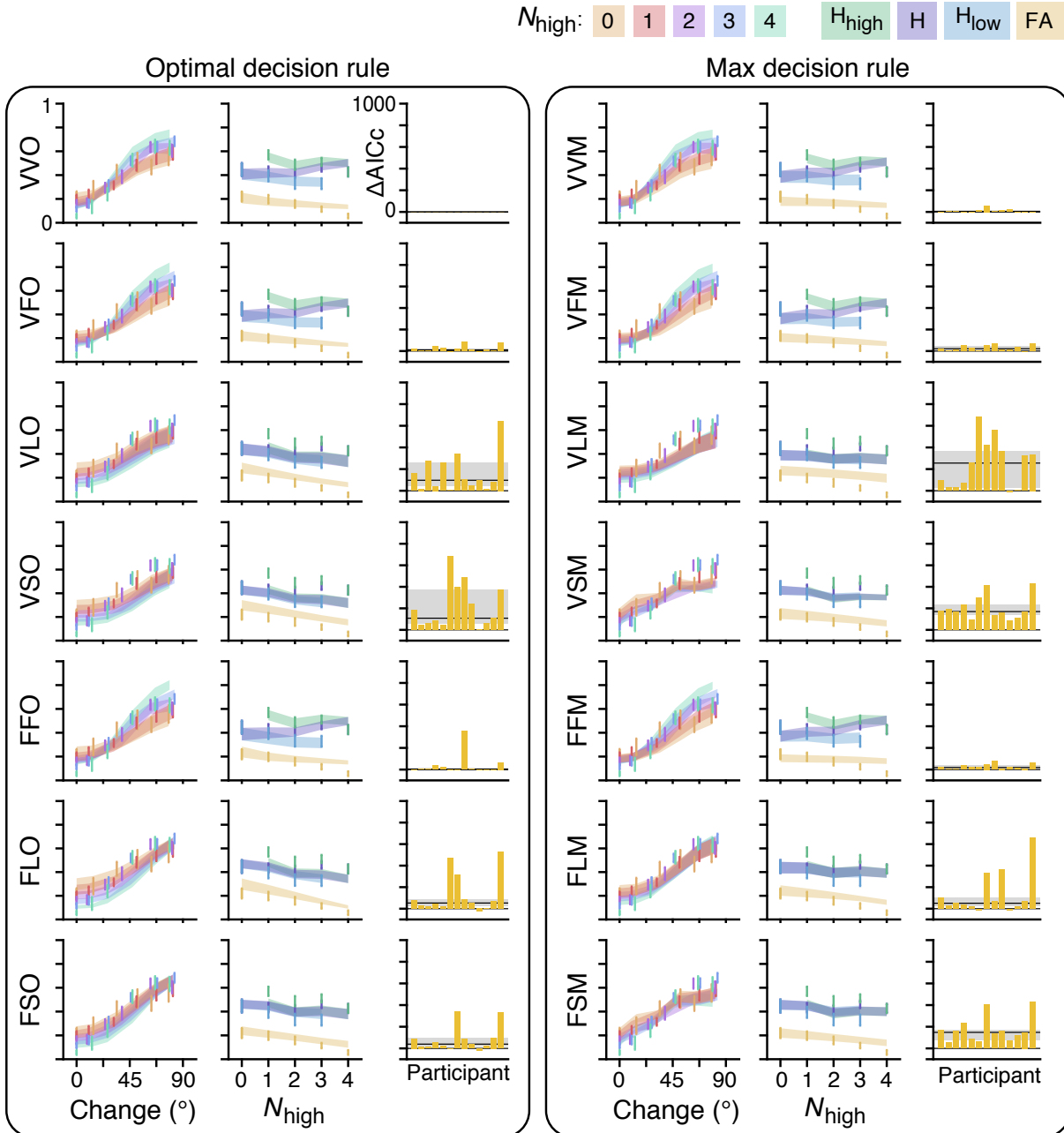


Figure 5: **Factorial model comparison.** Model predictions and performance of all possible combinations of different encoding, inference, and decision rules. $M \pm SEM$ data (error bars) and model fits (fills) for all models, organized into two columns by decision rule. For each model (each row within each column), the left graph illustrates the proportion report “change” as a function of amount of change. Color indicates the number of high-reliability ellipses (legend at the top of the figure). The middle graph illustrates the proportion hits for high-reliability items (green), hits for low-reliability items (blue), hits averaged across the display (purple), and false alarms (yellow) as a function of number of high-reliability items (legend at the top right of the figure). The right graph illustrates the individual-participant $\Delta AICc$, where positive numbers indicate the VVO model is a better fit to the data. The grey horizontal line and shaded region illustrates median and the 95% bootstrapped confidence interval of the median across participants.

405 6.5.2 Comparison of model families

406 A comparison of individual models did not provide a clear picture of what factor, or combination of factors is most
 407 important to describe human data best. To more directly address which factor contributes most to a model’s success,
 408 we define model families, where each family is a subset of all models that share a particular level of a particular factor,
 409 regardless of their levels of other factors (van den Berg et al., 2014; Shen & Ma, 2019). For example, all seven observer
 410 models that use an optimal decision rule would be included in the (O)ptimal level of the decision rule factor, regardless
 411 of their individual encoding or inference schemes. Similar to Shen & Ma, 2019, we compute the approximate marginal
 412 likelihood for level i for factor F , F_i . To calculate this value, we first marginalize over all of our tested models M :

$$L(F_i) = p(\text{data}|F_i) \approx \sum_M p(\text{data}|M)p(M|F_i). \quad (7)$$

413 Next, we assume that all models containing level i of factor F are a priori equally probable, so that

$$L(F_i) \approx \frac{1}{\text{number of models of level } i \text{ for factor } F} \sum_{F_i \text{ models}} p(\text{data}|M). \quad (8)$$

414 We approximate the log marginal likelihood of a given model with $-0.5 * AICc$ (Burnham & Anderson, 2002):

$$L(F_i) \approx \frac{1}{\text{number of models of level } i \text{ for factor } F} \sum_{F_i \text{ models}} e^{-.5AICc(M)}. \quad (9)$$

We define the *log level likelihood ratio* between level i and j as the ratio of their log marginal likelihoods:

$$\begin{aligned} LLLR_{AICc} &= \log \frac{p(\text{data}|F_i)}{p(\text{data}|F_j)} \quad (10) \\ &\approx \log \left(\sum_{F_1 \text{ models}} e^{-.5AICc(M)} \right) - \log \left(\sum_{F_2 \text{ models}} e^{-.5AICc(M)} \right) \\ &\quad + \log \left(\frac{\text{number of models of level } j \text{ for factor } F}{\text{number of models of level } i \text{ for factor } F} \right) \end{aligned}$$

415 We also compute $LLLR_{BIC}$, which approximates the log marginal likelihood of a given model with $-0.5BIC$, and
 416 more severely penalizes models with more parameters. To interpret the values for the LLLRs, we use Jeffrey’s scale,
 417 a common scale used when interpreting Bayes factors (Jeffreys, 1961).

418 **Model factor 1: encoding scheme.** The first model factor we explored is the observer’s encoding scheme. When
 419 using $LLLR_{AICc}$, there is weak support that (V)ariable precision encoding outperforms (F)ixed precision encoding
 420 (summed [95% bootstrapped confidence interval (CI)] 84 [0, 181]). However, there is no evidence when using
 421 $LLLR_{BIC}$ that either encoding scheme is favored (13 [-71, 116]). These results taken together imply weak and un-
 422 reliable evidence in favor of a variable precision encoding.

423 **Model factor 2: inference scheme.** The second model factor is the observer’s inference scheme. As with the
 424 encoding scheme, (V)ariable precision fits better than (F)ixed when using $AICc$ (105 [23, 200]), but not when using
 425 BIC (24 [-57, 126]). For both model comparison metrics, (L)imited and (S)ame inference schemes demonstrate a
 426 consistent lack of goodness of fit when compared to V (Limited – $AICc$: 500 [148, 928], BIC : 599 [253, 1047]; Same
 427 – $AICc$: 565 [204, 940], BIC : 565 [214, 974]) and F (Limited – $AICc$: 394 [68, 829], BIC : 575 [242, 996]) and Same:

428 (AICc: 460 [124, 874], BIC 541, [193, 996]) inference schemes. L and S inference schemes perform similarly (AICc:
429 66 [26, 105], BIC: -34 [-85, 15]). These results provide strong evidence that participants use either a V or F inference
430 scheme, but do not provide strong evidence to arbitrate between the two.

431 **Model factor 3: decision rule.** The third model factor is the observer's decision rule. There is moderate evidence
432 that the (O)ptimal decision rule fits better than the (M)ax decision rule when using BIC (69 [21, 132]) but not AICc
433 (41 [-2, 108]). This result provides inconclusive evidence that participants are using the optimal decision rule.

434 **Model factor 4: matching encoding and inference schemes.** Finally, we define the fourth factor as whether
435 encoding and inference schemes are matched (suggesting people have accurate representation of uncertainty) or mis-
436 matched (suggesting people do not have accurate representation of uncertainty). While the previous three factors each
437 investigate the effect of one model dimension on goodness-of-fit, this factor explores how the relationship between two
438 model dimensions affect goodness-of-fit. This factor is arguably the most important aspect of the model in addressing
439 our question of whether people maintain and use their uncertainty accurately over a working memory delay. The four
440 models with matching encoding and inference schemes are VVO, VVM, FFO, and FFM, and the remaining 10 models
441 are included in an "inference mismatched" level. There is very strong evidence that models where the inference and
442 encoding schemes match fit data better than models that do not have encoding-matched inference schemes (AICc: 136
443 [51, 237], BIC: 200 [124, 291]). This result provides strong support that people accurately represent their uncertainty
444 when completing the change detection task.

445 7 Discussion

446 In this paper, we investigated whether uncertainty is maintained and implicitly used in a working memory-based deci-
447 sion. First, we demonstrated through the Ellipse condition that people use uncertainty implicitly in a working memory
448 task if that uncertainty information was available after the delay (i.e., if uncertainty did not need to be maintained).
449 Second and more importantly, we showed through the Line condition that people not only use uncertainty, but main-
450 tain this information over the working memory delay. Finally, we factorially tested different model encoding schemes,
451 inference schemes, and decision rules and found that people were indeed best described by models in which observers
452 accurately maintain and use uncertainty in their decision.

453 First, we demonstrated through the Ellipse condition that people could use uncertainty implicitly in a working
454 memory task if that uncertainty information was experimentally available. While the change detection task has been
455 an experimental staple in the working memory literature (e.g., Luck & Vogel, 1997; Phillips, 1974; Pashler, 1988),
456 the majority of these tasks feature large, categorical changes in the stimulus. In contrast, our task, which is a direct
457 experimental replication of that of Keshvari and others (2012), featured changes that varied on a trial-to-trial basis.
458 Trial-to-trial fluctuations in stimuli and withholding of feedback allow for a strongest test of probabilistic computation
459 because observers would need to maintain a belief distribution over stimulus values to maximize performance in
460 this task (Ma & Jazayeri, 2014). Through formal model comparison, we showed that all participants in the Ellipse
461 condition are better fit by the Use Uncertainty model than the Ignore Uncertainty model. The Use Uncertainty model

462 was identical to the model that was found to describe participant data best in the study by Keshvari et al. (2012). These
463 results are also theoretically consistent with Devkar and others' (2017) work, despite being slightly different tasks.

464 Second and more importantly, we showed through the Line condition that people not only use uncertainty, but
465 maintain this information over the working memory delay. Like in the Ellipse condition, we found that all participants
466 in the Line condition were better fit by the Use Uncertainty model than the Ignore Uncertainty model. However, the
467 conclusion of this model comparison is critically different. In the Ellipse condition as well as in previous studies
468 (Keshvari et al., 2012; Devkar et al., 2017), the ellipses were presented after the working memory delay, with the
469 same reliability as before. With these experimental designs, reliability information could be used as a heuristic to
470 inform uncertainty, thus not requiring this information to be maintained in memory. In other words, these previous
471 studies cannot make any conclusions about the contents of working memory, only the decision-making process that
472 follows it. Our result, in contrast, demonstrates that uncertainty was actually *maintained* in working memory, since
473 the information was not available to the participants at the decision time through a heuristic such as ellipse reliability.

474 Finally, we conducted a factorial model comparison to investigate whether our conclusions were due to specific
475 assumptions about model encoding schemes, inference schemes, and decision rules. When comparing individual mod-
476 els, models with different combinations of Variable or Fixed precision encoding scheme, Variable or Fixed precision
477 inference scheme, and Optimal or Max decision rule were able to fit the data well. When comparing model fami-
478 lies, we found that the only factor that clearly determined the goodness of fit of a model was whether the encoding
479 and inference schemes were matched; only models with matching encoding and inference schemes captured human
480 behavior qualitatively well, and these models were quantitatively superior to those without matching encoding and
481 inference schemes. We thus conclude that the most important aspect of the model is that the observer accurately uses
482 their uncertainty in the change detection decision, not the specifics of the encoding or inference process.

483 The results of this study corroborate those of previous studies, and extend them by providing evidence that people
484 maintain uncertainty and use it *implicitly* and in a way that is *behaviorally-beneficial*. This is in contrast to studies
485 that asked participants to make explicit reports such as confidence ratings (Rademaker et al., 2012; Vandenbroucke
486 et al., 2014; Samaha & Postle, 2017), because use of uncertainty in these tasks are neither implicit nor behaviorally
487 beneficial (i.e., your confidence rating doesn't affect your performance). Tasks such as the "choose best" (Fougnie
488 et al., 2012; Suchow et al., 2017) and wager paradigms (Yoo et al., 2018; Honig et al., 2020) use uncertainty in a
489 performance-relevant way, but it is arguable whether this use of uncertainty is implicit. These tasks can be considered
490 implicit in the sense that there is a nontrivial mapping from uncertainty to performance-maximizing behavior in a post-
491 perceptual decision, but explicit in the sense that this decision is related to a conscious feeling of trust in a memory.
492 Conversely, a whole-report experiment by Adam and others (2017) analyzed by Schneegans and others (2020) clearly
493 demonstrates an implicit use of uncertainty by showing participants reported remembered items in decreasing order of
494 memory precision. However, unlike in our study, this use was not behaviorally beneficial; Adam and colleagues found
495 a nonsignificant performance difference when allowing participants to freely report versus being probed on which
496 items to report their memory of.

497 A typical, and reasonable, criticism of psychophysical experiments like the one presented in this paper is whether

498 it can successfully distinguish whether people are representing uncertainty per se or some stimulus feature (i.e., ellipse
499 reliability) as a *proxy* for it. Because observers with a Variable precision inference scheme represent uncertainty that
500 fluctuates above and beyond stimulus variability, it seems unlikely that this observer would be representing uncertainty
501 through stimulus reliability alone. This is, however, a valid criticism of the Fixed precision inference observer because
502 the variability of their uncertainty representation fluctuates with stimulus reliability. While we did not directly test this
503 alternative explanation (e.g., Barthelmé & Mamassian, 2010), we do not believe this criticism trivializes our results.

504 First, our results do not provide any evidence that people are simply maintaining ellipse reliability as a proxy for
505 uncertainty. If stimulus reliability was used as a proxy for uncertainty, then models with a Fixed precision inference
506 scheme would explain data best, independent of the encoding scheme. Instead, we found that the most important
507 aspect of our models' goodness of fit was that the encoding and inference schemes were *matched*, suggesting that
508 accurate representation of uncertainty is the most important aspect to explaining human behavior.

509 Second, performing this task while maintaining a proxy to uncertainty is not as trivial as it may initially seem.
510 Participants would still have to maintain this proxy to uncertainty over the working memory delay, then map this value
511 to their decision rule in a way consistent with an optimal Bayesian observer. Since participants were not provided
512 feedback on their performance, it is not obvious how they would have learned this mapping throughout the exper-
513 iment. It is still possible that people do indeed map a stimulus feature to a decision in a way that is behaviorally
514 and computationally indistinguishable from representing uncertainty itself. We do not believe this explanation would
515 trivialize our results; either explanation still allows us to conclude that people maintain uncertainty (or a proxy of it)
516 across a working memory delay, and use it implicitly in a task to improve performance.

517 Our results suggest that existing computational models of working memory that currently ignore uncertainty should
518 be updated. For example, attractor network models currently maintain a point estimate of a single item feature through
519 the mean of a stereotyped bump in a network of neurons (Ermentrout, 1998; Wang, 2001; Compte, 2006). Thus,
520 there is typically no notion of uncertainty in this framework. Lim and Goldman (2014) demonstrated that altering the
521 network connectivity and dynamics results in “negative-derivative feedback models,” in which networks can vary not
522 only in mean but also in amplitude. Probabilistic population coding (PPC) and neural network models have imple-
523 mented precision through input gain (Ma, Beck, Latham, & Pouget, 2006; Orhan & Ma, 2017). Additional research
524 must investigate whether these negative-derivative feedback models can represent a memory's precision through the
525 amplitude of the network maintaining it, precision which could be read out from the observer as uncertainty.

526 Additionally, computational models could be used to decode uncertainty from neural activity in working memory
527 tasks. Work in visual perception demonstrates that uncertainty information is represented in primary visual cortex (van
528 Bergen, Ma, Pratte, & Jehee, 2015; van Bergen, 2019; Walker, Cotton, Ma, & Tolia, 2020; Hénaff, Boundy-Singer,
529 Meding, Ziemba, & Goris, 2020). These studies built normative Bayesian models to infer stimulus value from fMRI
530 BOLD signal. The likelihood of the stimulus, and thus uncertainty, could be read out from the models. Estimates
531 of trial-specific uncertainty are positively correlated with error, suggesting that primary visual cortex held uncertainty
532 information. Since working memories have been shown to be maintained in the same sensory areas with which they
533 are perceived (e.g. Curtis & D'Esposito, 2003; Postle, 2006; D'Esposito & Postle, 2015; Harrison & Tong, 2009),

534 perhaps visual working memory uncertainty is also stored in visual cortex. To more rigorously test the representation
535 of uncertainty decoded from BOLD data, future studies can correlate decoded uncertainty with behavioral measures of
536 uncertainty such as confidence ratings (Rademaker et al., 2012) or post-decision wagers (Yoo et al., 2018; Honig et al.,
537 2020). Additionally, future studies can try to fit individual-trial data using these methods, which is more compelling
538 evidence in favor of a model than a correlation.

539 Overall, this paper shows that people have uncertainty that reflects their memory noise at an item-specific level
540 and they maintain this information over a working memory delay. This research demonstrates that there is other
541 information, beyond a point estimate, maintained in working memory and used in later decisions.

542 **Acknowledgements:** We thank Marissa Evans for the massive help collecting data for this study and Emin Orhan for
543 collaborating on a previous iteration of this project. W.J.M is supported by award number R01EY020958. A.H.Y. was
544 supported by training grant T32 EY7136-25. This work was supported in part through the NYU IT High Performance
545 Computing resources, services, and staff expertise.

References

- 546
- 547 Acerbi, L., & Ma, W. J. (2017). Practical Bayesian optimization for model fitting with Bayesian Adaptive Direct
548 Search. *Advances in Neural Information Processing Systems*, *30*, 1836–1846.
- 549 Acerbi, L., Vijayakumar, S., & Wolpert, D. M. (2014). On the origins of suboptimality in human probabilistic
550 inference. *PLoS Computational Biology*, *10*(6), e1003661. doi: 10.1371/journal.pcbi.1003661
- 551 Acerbi, L., Wolpert, D. M., & Vijayakumar, S. (2012). Internal representations of temporal statistics and feedback
552 calibrate motor-sensory interval timing. *PLoS Computational Biology*, *8*(11), e1002771. doi: 10.1371/journal
553 .pcbi.1002771
- 554 Adam, K. C. S., & Vogel, E. K. (2017). Confident failures: Lapses of working memory reveal a metacognitive blind
555 spot. *Attention, Perception & Psychophysics*, *79*(5), 1506–1523. doi: 10.3758/s13414-017-1331-8
- 556 Adam, K. C. S., Vogel, E. K., & Awh, E. (2017). Clear evidence for item limits in visual working memory. *Cognitive*
557 *Psychology*, *97*, 79–97. doi: 10.1016/j.cogpsych.2017.07.001
- 558 Alais, D., & Burr, D. (2004). The ventriloquist effect results from near-optimal bimodal integration. *Current Biology*,
559 *14*(3), 257–262. doi: 10.1016/j.cub.2004.01.029
- 560 Baddeley, A. D. (2003). Working memory: Looking back and looking forward. *Nature Reviews Neuroscience*, *4*,
561 829–839. doi: 10.1038/nrn1201
- 562 Baddeley, A. D., & Hitch, G. (1974). Working memory. *The Psychology of Learning and Motivation*, *8*, 47–89. doi:
563 10.1016/S0079-7421(08)60452-1
- 564 Barthelmé, S., & Mamassian, P. (2010). Flexible mechanisms underlie the evaluation of visual confidence. *Pro-*
565 *ceedings of the National Academy of Sciences of the United States of America*, *107*(48), 20834–20839. doi:
566 10.1073/pnas.1007704107
- 567 Bays, M. P., & Husain, M. (2008). Dynamic shifts of limited working memory resources in human vision. *Science*,
568 *321*(5890), 851–854. doi: 10.1126/science.1158023
- 569 Beck, J. M., Ma, W. J., Pitkow, X., Latham, P. E., & Pouget, A. (2012). Not noisy, just wrong: The role of suboptimal
570 inference in behavioral variability. *Neuron*, *74*(1), 30–39. doi: 10.1016/j.neuron.2012.03.016
- 571 Bona, S., Cattaneo, Z., Vecchi, T., Soto, D., & Silvanto, J. (2013). Metacognition of Visual Short-Term Memory:
572 Dissociation between objective and subjective components of VSTM. *Frontiers in Psychology*, *4*(62). doi:
573 10.3389/fpsyg.2013.00062
- 574 Bona, S., & Silvanto, J. (2014). Accuracy and confidence of visual short-term memory do not go hand-in-hand:
575 Behavioral and neural dissociations. *PLoS ONE*, *9*(3), e90808. doi: 10.1371/journal.pone.0090808
- 576 Burnham, K. P., & Anderson, D. R. (2002). *Model selection and inference: A practical information-heuristic approach*
577 (2nd ed.). New York, NY: Springer-Verlag.
- 578 Compte, A. (2006). Computational and in vitro studies of persistent activity: Edging towards cellular and synaptic
579 mechanisms of working memory. *Neuroscience*, *139*(1), 135–151. doi: 10.1016/j.neuroscience.2005.06.011
- 580 Conway, A. R. A., Kane, M. J., & Engle, R. W. (2003). Working memory capacity and its relation to general
581 intelligence. *Trends in Cognitive Sciences*, *7*(12), 547–552. doi: 10.1016/j.tics.2003.10.005

- 582 Curtis, C. E., & D'Esposito, M. (2003). Persistent activity in the prefrontal cortex during working memory. *Trends in*
583 *Cognitive Sciences*, 7(9), 415–423. doi: 10.1016/S1364-6613(03)00197-9
- 584 D'Esposito, M., & Postle, B. R. (2015). The cognitive neuroscience of working memory. *Annual Review of Psychol-*
585 *ogy*, 66, 115–142. doi: 10.1146/annurev-psych-010814-015031
- 586 Devkar, D., Wright, A. A., & Ma, W. J. (2017). Monkeys and humans take local uncertainty into account when
587 localizing a change. *Journal of Vision*, 17(11). doi: 10.1167/17.11.4
- 588 Ermentrout, B. (1998). Neural networks as spatio-temporal pattern-forming systems. *Reports on Progress in Physics*,
589 61(4), 353–430. doi: 10.1088/0034-4885/61/4/002
- 590 Ernst, M. O., & Banks, M. S. (2002). Humans integrate visual and haptic information in a statistically optimal fashion.
591 *Nature*, 415(6870), 429–433. doi: 10.1038/415429a
- 592 Fougnie, D., Suchow, J. W., & Alvarez, G. A. (2012). Variability in the quality of visual working memory. *Nature*
593 *Communications*, 3, 1229. doi: 10.1038/ncomms2237
- 594 Fukuda, K., Vogel, E., Mayr, U., & Awh, E. (2010). Quantity, not quality: The relationship between fluid intelligence
595 and working memory capacity. *Psychonomic Bulletin & Review*, 17(5), 673–679. doi: 10.3758/17.5.673
- 596 Green, D., & Swets, J. A. (1966). *Signal detection theory and psychophysics*. Wiley.
- 597 Harrison, S. A., & Tong, F. (2009). Decoding reveals the contents of visual working memory in early visual areas.
598 *Nature*, 458(7238), 632–635. doi: 10.1038/nature07832
- 599 Hénaff, O. J., Boundy-Singer, Z. M., Meding, K., Ziemba, C. M., & Goris, R. L. T. (2020). Representation of visual
600 uncertainty through neural gain variability. *Nature Communications*, 11, 2513. doi: 10.1038/s41467-020-15533
601 -0
- 602 Honig, M., Ma, W. J., & Fougnie, D. (2020). Humans incorporate trial-to-trial working memory uncertainty into
603 rewarded decisions. *Proceedings of the National Academy of Sciences of the United States of America*, 117(15),
604 8391–8397. doi: 10.1073/pnas.1918143117
- 605 Hurvich, C. M., & Tsai, C. L. (1987). Regression and time series model selection in small samples. *Biometrika*, 76(2),
606 297–307. doi: 10.1093/biomet/76.2.297
- 607 Jazayeri, M., & Shadlen, N. M. (2010). Temporal context calibrates interval timing. *Nature Neuroscience*, 13(8),
608 1020–1026. doi: 10.1038/nn.2590
- 609 Jeffreys, H. (1961). *Theory of probability (3rd ed.)*. New York: Oxford University Press.
- 610 Just, M. A., & Carpenter, P. A. (1992). A capacity theory of comprehension: Individual differences in working
611 memory. *Psychological review*, 99(1), 122–149. doi: 10.1037/0033-295X.99.1.122
- 612 Keshvari, S., van den Berg, R., & Ma, W. J. (2012). Probabilistic computation in human perception under variability
613 in encoding precision. *PLoS ONE*, 7.
- 614 Knill, D. C., & Pouget, A. (2004). The Bayesian brain: The role of uncertainty in neural coding and computation.
615 *Trends in Neurosciences*, 27(12), 712–719. doi: 10.1016/j.tins.2004.10.007
- 616 Körding, P. K., & Wolpert, D. M. (2004). Bayesian integration in sensorimotor learning. *Nature*, 427, 244–247. doi:
617 10.1038/nature02169

- 618 Lim, S., & Goldman, M. S. (2014). Balanced cortical microcircuitry for spatial working memory based on corrective
619 feedback control. *Journal of Neuroscience*, *34*(20), 6790–6806. doi: 10.1523/JNEUROSCI.4602-13.2014
- 620 Luck, S. J., & Vogel, E. K. (1997). The capacity of visual working memory for features and conjunctions. *Nature*,
621 *390*, 279–281. doi: 10.1038/36846
- 622 Ma, W. J. (2010). Signal detection theory, uncertainty, and Poisson-like population codes. *Vision Research*, *50*(22),
623 2308–2319. doi: 10.1016/j.visres.2010.08.035
- 624 Ma, W. J. (2019). Bayesian decision models: A primer. *Neuron*, *104*, 164–175. doi: 10.1016/j.neuron.2019.09.037
- 625 Ma, W. J., Beck, J. M., Latham, P. E., & Pouget, A. (2006). Bayesian inference with probabilistic population codes.
626 *Nature Neuroscience*, *9*, 1432–1438. doi: 10.1038/nn1790
- 627 Ma, W. J., & Jazayeri, M. (2014). Neural coding of uncertainty and probability. *Annual review of neuroscience*, *37*,
628 205–220. doi: 10.1146/annurev-neuro-071013-014017
- 629 Ma, W. J., Navalpakkam, V., Beck, M. J., van den Berg, R., & Pouget, A. (2011). Behavior and neural basis of
630 near-optimal visual search. *Nature Neuroscience*, *14*(6), 783–90.
- 631 Ma, W. J., Shen, S., Dziugaite, G., & van den Berg, R. (2015). Requiem for the max rule? *Vision Research*, *116*,
632 179–193. doi: 10.1016/j.visres.2014.12.019
- 633 Maloney, L. T., & Mamassian, P. (2009). Bayesian decision theory as a model of human visual perception: Testing
634 Bayesian transfer. *Visual Neuroscience*, *26*(1), 147–155. doi: 10.1017/S0952523808080905
- 635 Maloney, L. T., & Zhang, H. (2010). Decision-theoretic models of visual perception and action. *Vision Research*,
636 *50*(23), 2362–2374. doi: 10.1016/j.visres.2010.09.031
- 637 Maniscalco, B., & Lau, H. (2015). Manipulation of working memory contents selectively impairs metacognitive
638 sensitivity in a concurrent visual discrimination task. *Neuroscience of consciousness*, *2015*(1), niv002. doi:
639 10.1093/nc/niv002
- 640 Mueller, S. T., & Weidemann, C. T. (2008). Decision noise: An explanation for observed violations of signal detection
641 theory. *Psychonomic Bulletin & Review*, *15*(3), 465–494. doi: 10.3758/PBR.15.3.465
- 642 Orhan, A. E., & Jacobs, R. A. (2014). Are performance limitations in visual short-term memory tasks due to capacity
643 limitations or model mismatch? *arXiv*.
- 644 Orhan, A. E., & Ma, W. J. (2017). Efficient probabilistic inference in generic neural networks trained with non-
645 probabalistic feedback. *Nature Communications*, *8*(1), 138. doi: 10.1038/s41467-017-00181-8
- 646 Pashler, H. (1988). Familiarity and visual change detection. *Perception & Psychophysics*, *44*, 369–378. doi: 10.3758/
647 BF03210419
- 648 Phillips, A. W. (1974). On the distinction between sensory storage and short-term visual memory. *Perception &*
649 *Psychophysics*, *16*, 283–290. doi: 10.3758/BF03203943
- 650 Postle, B. R. (2006). Working memory as an emergent property of the mind and brain. *Neuroscience*, *139*(1), 23–38.
651 doi: 10.1016/j.neuroscience.2005.06.005
- 652 Rademaker, R. L., Tredway, C. H., & Tong, F. (2012). Introspective judgments predict the precision and likelihood of
653 successful maintenance of visual working memory. *Journal of Vision*, *12*(13), 21. doi: 10.1167/12.13.21

- 654 Sahar, T., Sidi, Y., & Makovski, T. (2020). A metacognitive perspective of visual working memory with rich complex
655 objects. *Frontiers in Psychology, 11*, 179. doi: 10.3389/fpsyg.2020.00179
- 656 Samaha, J., Barrett, J. J., Sheldon, D. A., LaRocque, J. J., & Postle, B. R. (2016). Dissociating perceptual confidence
657 from discrimination accuracy reveals no influence of metacognitive awareness on working memory. *Frontiers*
658 *in Psychology, 7*, 851. doi: 10.3389/fpsyg.2016.00851
- 659 Samaha, J., & Postle, B. R. (2017). Correlated individual differences suggest a common mechanism underlying
660 metacognition in visual perception and visual short-term memory. *Proceedings of The Royal Society B Biologi-*
661 *cal Sciences, 284*(1867), 20172035. doi: 10.1098/rspb.2017.2035
- 662 Schneegans, S., Taylor, R., & Bays, P. M. (2020). Stochastic sampling provides a unifying account of visual working
663 memory limits. *Proceedings of the National Academy of Sciences of the United States of America, 117*(34),
664 20959-20968. doi: 10.1073/pnas.2004306117
- 665 Schwarz, G. (1978). Estimating the dimension of a model. *The Annals of Statistics, 6*(2), 461–464. doi: 10.1214/aos/
666 1176344136
- 667 Shen, S., & Ma, W. J. (2019). Variable precision in visual perception. *Psychological review, 126*(1), 89-132. doi:
668 10.1037/rev0000128
- 669 Stephan, K. E., Penny, W. D., Daunizeau, J., Moran, R. J., & Friston, K. J. (2009). Bayesian model selection for group
670 studies. *NeuroImage, 46*.
- 671 Stocker, A. A., & Simoncelli, P. E. (2006). Noise characteristics and prior expectations in human visual speed
672 perception. *Nature Neuroscience, 9*, 578–585. doi: doi.org/10.1038/nn1669
- 673 Suchow, J. W., Fougny, D., & Alvarez, G. A. (2017). Looking inward and back: Real-time monitoring of visual
674 working memories. *Journal of Experimental Psychology. Learning, Memory, and Cognition, 43*(4), 660–668.
675 doi: 10.1037/xlm0000320
- 676 van Beers, J. R., Sittig, C. A., & Gon, J. J. (1999). Integration of proprioceptive and visual position-information:
677 An experimentally supported model. *Journal of neurophysiology, 81*(3), 1355–1364. doi: 10.1152/jn.1999.81
678 .3.1355
- 679 van Bergen, R. S. (2019). Probabilistic representation in human visual cortex reflects uncertainty in serial decisions.
680 *Journal of Neuroscience, 39*(41), 8164–8176. doi: 10.1523/JNEUROSCI.3212-18.2019
- 681 van Bergen, R. S., Ma, W. J., Pratte, M. S., & Jehee, J. F. (2015). Sensory uncertainty decoded from visual cortex
682 predicts behavior. *Nature Neuroscience, 17*28–1730. doi: 10.1038/nn.4150
- 683 van den Berg, R., Awh, E., & Ma, W. J. (2014). Factorial comparison of working memory models. *Psychological*
684 *Review, 121*(1), 124–149. doi: 10.1037/a0035234
- 685 van den Berg, R., Shin, H., Chou, W. C., George, R., & Ma, W. J. (2012). Variability in encoding precision accounts
686 for visual short-term memory limitations. *Proceedings of the National Academy of Sciences of the United States*
687 *of America, 109*(22), 8780–8785. doi: 10.1073/pnas.1117465109
- 688 van den Berg, R., Yoo, A. H., & Ma, W. J. (2017). Fechner’s law in metacognition: A quantitative model of visual
689 working memory confidence. *Psychological Review, 124*(2), 197–214. doi: 10.1037/rev0000060

- 690 Vandembroucke, E. A. R., Sligte, I. G., Barrett, A. B., Seth, A. K., Fahrenfort, J. J., & Lamme, V. A. (2014).
691 Accurate metacognition for visual sensory memory representations. *Psychological science*, 25(4), 861-873.
692 doi: 10.1177/0956797613516146
- 693 van Opheusden, B., Acerbi, L., & Ma, W. J. (2020). Unbiased and efficient log-likelihood estimation with Inverse
694 Binomial Sampling. *PLoS Computational Biology*, 16(12), e1008483. doi: 10.1371/journal.pcbi.1008483
- 695 Vlassova, A., Donkin, C., & Pearson, J. (2014). Unconscious information changes decision accuracy but not con-
696 fidence. *Proceedings of the National Academy of Sciences of the United States of America*, 111(45), 16214–
697 16218. doi: 10.1073/pnas.1403619111
- 698 Walker, E., Cotton, J., Ma, W. J., & Tolias, A. (2020). A neural basis of probabilistic computation in visual cortex.
699 *Nature Neuroscience*, 23, 122–129. doi: 10.1038/s41593-019-0554-5
- 700 Wang, X. J. (2001). Synaptic reverberation underlying mnemonic persistent activity. *Trends in Neurosciences*, 24(8),
701 455–463. doi: 10.1016/s0166-2236(00)01868-3
- 702 Yoo, A. H., Klyszejko, Z., Curtis, E. C., & Ma, W. J. (2018). Strategic allocation of working memory resource.
703 *Scientific Reports*, 8, 16162. doi: 10.1038/s41598-018-34282-1
- 704 Zhang, W., & Luck, J. S. (2008). Discrete fixed-resolution representations in visual working memory. *Nature*, 453,
705 233–235. doi: 10.1038/nature06860